JOURNAL OF MATERIALS SCIENCE **36** (2001) 441–450

Reinforcement of molten carbonate fuel cell matrixes by adding rod-shaped γ-LiAlO$_2$ particles

S. H. HYUN*, S. C. CHO, J. Y. CHO, D. H. KO
School of Materials Science and Engineering, College of Engineering, Yonsei University, Seoul 120-749, South Korea
E-mail: prohsh@yonsei.ac.kr

S. A. HONG
Battery & Fuel Cell Research Center, KIST, Seoul 136-791, South Korea

Improvement in strength of γ-LiAlO$_2$ matrixes for a molten carbonate fuel cell (MCFC) via addition of rod-shaped γ-LiAlO$_2$ particles has been investigated. The rod-shaped γ-LiAlO$_2$ particles with the aspect ratio of 9–15 were obtained by heat-treating rod-shaped β-LiAlO$_2$ particles at 800 °C for 3 h, synthesized from the reaction mixture of LiOH-γ-Al$_2$O$_3$-NaOH. The γ-form was very stable for more than 700 h in a molten carbonate environment at 650 °C, while the β-form showed both a phase change from β- to γ-LiAlO$_2$ and a morphology change from rod- to bipyramid-shapes. The average pore size and the porosity of the matrix (550 μm thickness) fabricated by tape-casting of the slurry with weight ratio 1.0 of rod-shaped γ-LiAlO$_2$ particles to commercial γ-LiAlO$_2$ powders (2.0 μm dia.) were about 0.12 μm and 54%, respectively, after being heat-treated at 650 °C for 2 h. The strength (197 g$_f$/mm^2) of the rod- shaped particle reinforced matrixes was enhanced more than twice as much as that of the non-reinforced γ-LiAlO$_2$ matrixes (91 g$_f$/mm^2). © *2001 Kluwer Academic Publishers*

1. Introduction

The molten carbonate fuel cell (MCFC) is one of the most attractive methods for future electric power generation. The MCFC has great advantages, such as very high electrochemical conversion efficiency and pollution free operation, but a lot of improvements in the MCFC operating life-time and efficiency are still required for its commercialization. The component materials of construction for the fuel cell stack operated at the high temperature of 650 °C are of prime importance. In particular, the matrix which contains the very reactive electrolyte like alkali molten carbonates should be inert as well as stable for electrolyte retention [1–3]. Therefore, the MCFC matrixes have been usually fabricated to have a porosity of 50–60% and a pore size below 1 μm using γ-LiAlO$_2$ which is known to be very stable for molten carbonates [4]. Another important property of the matrix is the mechanical strength to maintain structural integrity under stacking load, especially during the thermal cycle.

Materials for reinforcing the MCFC matrix should not only be inert to molten carbonates but also free from phase transition/microstructure change even for a long period of operation at the high temperature of 650 °C. Alumina fiber-reinforcements were attempted to improve the mechanical properties of the γ-LiAlO$_2$ matrixes [2, 5]. Since alumina fibers were not stable with molten carbonates in the environment as MCFC, it has been revealed that the fiber-addition caused the cell performance to decay gradually with running time. On the other hand, some limited researches on reinforcements of γ-LiAlO$_2$ matrix by adding alumina fibers coated with γ-LiAlO$_2$ or γ-LiAlO$_2$ fibers [2, 6, 7] have been conducted to minimize the corrosion problems. It is basically believed that these types of fiber may provide the desired strengthening of the matrix, but the result of these fiber-reinforcements on the fuel cell performance has not been clearly explained yet. An improvement in matrix strength via addition of a second phase crack arrestors like large γ-LiAlO$_2$ particles has also been sought [8]. Although some improvements have been achieved by the above methods, further improvement in matrix strength/thermal cycleability may be desirable to meet the commercialization requirements of the MCFC system.

In recent years, rod-/needle-shaped γ-LiAlO$_2$ single crystals superior to polycrystalline fibers in points of their chemical and thermal stability and mechanical strength have been extensively considered as a new material for reinforcing the MCFC matrix [9, 10]. Besides their property excellence, rod-shaped single crystals may be easily manufactured in comparison with the fiber [11, 12], and also be uniformly dispersed inside the matrix even via tape casting. However, the actual

---

* Author to whom all correspondence should be addressed.

performance of the MCFC matrix reinforced by the addition of rod-shaped γ-$LiAlO_2$ particles is still open to question.

In this work, the high strength γ-$LiAlO_2$ matrix for MCFC has been developed via the addition of rod-shaped γ-$LiAlO_2$ particles as reinforcing materials prepared by heat-treating rod-shaped β-$LiAlO_2$ crystals synthesized from the reaction mixture of LiOH-γ-Al_2O_3-NaOH. The phase/morphology stability and the corrosion resistance of $LiAlO_2$ were evaluated from results obtained by a corrosion test in alkali molten carbonates, and the microstructure and mechanical strength of reinforced γ-$LiAlO_2$ matrixes are also discussed.

2. Experimental procedure

2.1. Synthesis of rod-shaped β-/γ-$LiAlO_2$ crystals

The overall experimental flow chart for this study on reinforcing the MCFC matrix by adding rod-shaped γ-$LiAlO_2$ particles is given in Fig. 1, and the detailed experimental procedure in each step is as below.

The crystal phase of $LiAlO_2$ can be obtained in various forms depending on reaction conditions and starting materials. In this work, the formation reaction of the rod-shaped β-$LiAlO_2$ crystal at relatively low temperature was based on the following reaction suggested by Kinoshita *et al.* [11].

$$2LiOH + Al_2O_3 = 2LiAlO_2 + H_2O \qquad (1)$$

$LiOH{\cdot}H_2O$ (Junsei Co.) and γ-Al_2O_3 (Aldrich Co.) were used as sources of LiOH and Al_2O_3, respectively, and NaOH (Junsei Co.) as flux and reaction promoter. The compositions of the reaction mixture used for controlling the aspect ratio of rod-shaped particles is given in Table I. The rod-shaped β-$LiAlO_2$ was crystallized by heat-treating the slurry of DI water (30 wt%) and the reaction mixture (70 wt%) of Table I in an alumina crucible at 200–700 °C for 3–20 h. The heating rate was 1–5 °C/min. The final rod-shaped β-$LiAlO_2$ particles were obtained after removing NaOH and residual soluble components via washing the reacted mixture with DI water for 24 h.

TABLE I Compositions of reaction mixtures for synthesizing rod-shaped β-$LiAlO_2$ crystals

Specimen No.	Mole ratio ($LiOH{\cdot}H_2O$: γ-Al_2O_3 : Na OH)	Mole ratio ($LiOH{\cdot}H_2O$/ γ-Al_2O_3)	NaOH content (mole %)
1	3.33 : 1.67 : 5.00	2.0	50
2	3.75 : 1.25 : 5.00	3.0	50
3	4.00 : 1.00 : 5.00	4.0	50
4	4.17 : 0.83 : 5.00	5.0	50
5	4.29 : 0.71 : 5.00	6.0	50
6	6.13 : 0.87 : 3.00	7.0	30
7	5.25 : 0.75 : 4.00	7.0	40
8	4.38 : 0.62 : 5.00	7.0	50
9	3.50 : 0.50 : 6.00	7.0	60
10	4.44 : 0.56 : 5.00	8.0	50

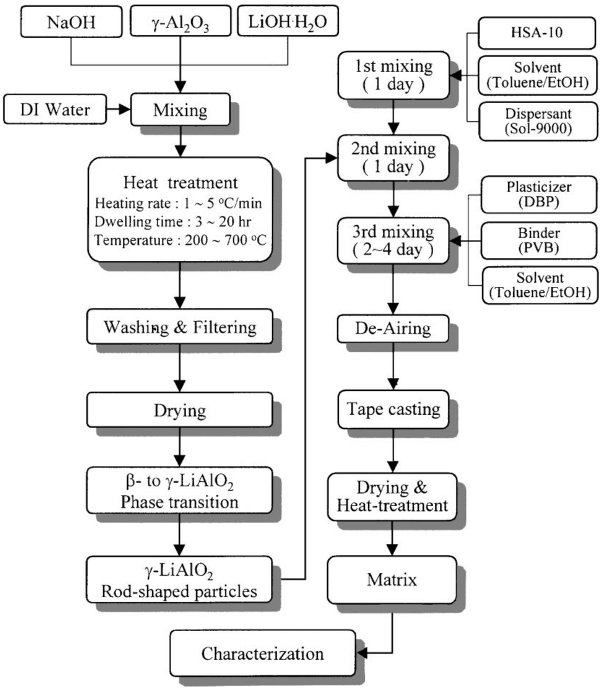

Figure 1 Overall experimental flow chart.

For the synthesis of γ-$LiAlO_2$ particles due to the phase transition of β to γ form, the rod-shaped β-$LiAlO_2$ particles were heat-treated in an alumina crucible with the top-cover or without the top-cover at 700–800 °C for 0.5–20 h. The crystalline phase was analyzed by XRD (Rint 2700, Rigaku) and the morphology and aspect ratio of rod-shaped particles were observed by SEM (H600, Hitachi).

2.2. Corrosion resistance of β-/γ-$LiAlO_2$ against molten carbonate

The corrosion testing was conducted to verify whether rod-shaped β-/γ-$LiAlO_2$ particles synthesized in this work could be used as an appropriate reinforcing material of the γ-$LiAlO_2$ matrix in the operation environment of MCFC. The corrosion tests were performed for powder samples immersed in molten carbonate of 650 °C for 24–700 h under ambient atmospheric pressure. For comparison, the commercial γ-$LiAlO_2$ powder (HSA-10, Cyprus Co.) used as a matrix material in this work was also tested. The same composition of the molten carbonate electrolyte (mole ratio of $Li_2CO_3/K_2CO_3 = 68/38$) as used in the actual MCFC unit cell test in our research group was utilized. After removing the carbonates remaining in the corrosion-tested samples by washing with the mixture solution of acetic acid (99%, Duksan Co.) and acetic anhydrate (99%, Duksan Co.), phase and morphology changes of each particle were analyzed by XRD and SEM, respectively.

2.3. Preparation of reinforced γ-$LiAlO_2$ matrixes

The MCFC matrixes were fabricated by tape-casting of the slurry consisting of organic solvent, additives, and solid constituents as commercial γ-$LiAlO_2$ particles

TABLE II Slurry composition for tape casting of reinforced γ-$LiAlO_2$ matrixes

	Solid	Solvent				
Materials	γ-$LiAlO_2$ powders (HSA-10) + Rod-shaped particles	Toluene	Ethyl alcohol	Binder Polyvinylbutyral	Plasticizer Dibutylphthalate	Dispersant Solsperse-9000
Content (wt%)	30.2 (Rod-shaped particle content = 0 ∼ 100 %)	36.9	15.8	7.5	9.0	0.6

(Cyprus Foote Mineral Co.) and rod-shaped γ-$LiAlO_2$ particles manufactured in this work. A mixture of toluene (99%, Samchun Co.) and ethyl alcohol (99%, Duksan) was used as a solvent (dispersent medium) instead of water because of the high reactivity of $LiAlO_2$ with water. Polyvinylbutyral (98%, Sigma Co.) as a binder, dibutylphthalate (99%, Junsei Co.) as a plasticizer, and solsperse-9000 (Imperial chemical Ind.) as a dispersant were employed. The slurry composition of these components for tape-casting of fiber-reinforced or fiber free γ-$LiAlO_2$ matrixes was optimized already and published in our previous paper [13]. Table II shows the slurry composition used in this work, which is the same as before except for the type of solid constituents. The fiber for reinforcing the matrix was replaced with rod-shaped particles, and only the HSA-10 type of commercial γ-$LiAlO_2$ powders of which the specific surface area and the average particle diameter are 10 m^2/g and 2 μm, respectively, was used as a basic matrix material. The content of rod-shaped particles in the final calcined matrix was varied to be in the range from 0 to 100 wt% for optimizing the reinforced MCFC matrix. Non-reinforced matrixes were also prepared from the slurry containing the solid mixture of 50 wt% HSA-10 particles and 50 wt% LSA-50 particles of low surface area 0.1 m^2/g and diameter 50 μm for comparison with the reinforced matrixes.

The green sheet of the matrix (5×5 cm^2) was fabricated to have thickness 500–600 μm by tape-casting of the slurry over a smooth polyethylene film using a doctor blade apparatus (double blade type) made by Korea Institute of Science and Technology. The details of slurry preparation, tape-casting procedure, and heating schedule for green sheets upto MCFC operation temperature 650 °C were described in previous papers [13, 14]. In order to optimize the ball milling time of the slurry, the morphology/aspect ratio change of rod-shaped particles with the milling time (3–5 d) was examined in the final matrixes prepared from the slurry containing 100% rod-shaped particles only as a solid component.

The morphology and microstructures of the reinforced matrixes were observed by SEM, and the porosity and the pore size distribution were determined by Mercury Porosimetry (Autopore II 9220, Micromeritics Co.). The flexural strength was examined for matrixes heat-treated at 650 °C for 2 h and expressed as a three-point bend strength calculated from Equation 2 using fracture loading P (g_f) determined at room temperature under conditions of 1 mm/min cross head velocity and 25 mm span distance by Bend Strength Tester (Model 1127, Instron Co.) with 2 kg load cell.

$$\sigma = \frac{3PL}{(2bd^2)} \tag{2}$$

In Equation 2, σ (g_f/mm^2) is three-point bend strength, L (mm) span distance, b (mm) specimen width, and d (mm) specimen thickness.

3. Results and discussion

3.1. Rod-shaped particles

3.1.1. Crystallization of β-$LiAlO_2$

The effect of the composition of the starting reaction mixture on β-$LiAlO_2$ crystallization and their morphology was examined by XRD and SEM. Fig. 2 shows the morphology change of reaction products depending on the molar ratio of $LiOH{\cdot}H_2O/\gamma$-Al_2O_3 in starting materials containing 50 mole % NaOH. The reaction mixtures were heated upto 600 °C at 5 °C/min, and then dwelled at that temperature for 3 h. As seen in Fig. 2a, although the mole ratio of 2.0 corresponds to the stoichiometric ratio of Equation 1, rod-shaped particles had not been formed. Furthermore, the reaction product was found to be not $LiAlO_2$ but mainly $Li_2Al_4(CO_3)(OH)_{12}{\cdot}3H_2O$ through XRD analysis. This result means that all of aluminum in the reaction mixture could not react completely with lithium under the given reaction conditions because of the low activity of lithium. As the mole ratio (i.e., amount of $LiOH{\cdot}H_2O$) increases, however, rod-shaped β-$LiAlO_2$ crystals start to appear in part, and finally only pure β-crystalline phase exists and all crystals have grown into rod-shapes when the molar ratio reaches above 7.0 as shown in Fig. 2e and f. It was concluded that the excess amount of $LiOH{\cdot}H_2O$ (mole ratio >7.0) should be added for all aluminum completely to react with lithium. Therefore, the synthesis of rod-shaped β-$LiAlO_2$ in this study hereafter was tried on the basis of starting materials having the $LiOH{\cdot}H_2O/\gamma$-Al_2O_3 mole ratio of 7.0.

In order to optimize the formation temperature of rod-shaped β-$LiAlO_2$ crystals, the crystalline phase and the morphology of reaction products obtained via heat-treating the reaction mixtures specified above at 200–700 °C for 3 h were analyzed by XRD (Fig. 3) and SEM (Fig. 4), respectively. Fig. 3 shows that the crystallization of β-$LiAlO_2$ starts even at 200 °C but its crystalline phase is fully developed at 600 °C. On the other hand, it was observed that β-crystalline phases were completely transformed into the γ-phase around 700 °C. The morphology of the reaction product changed gradually into

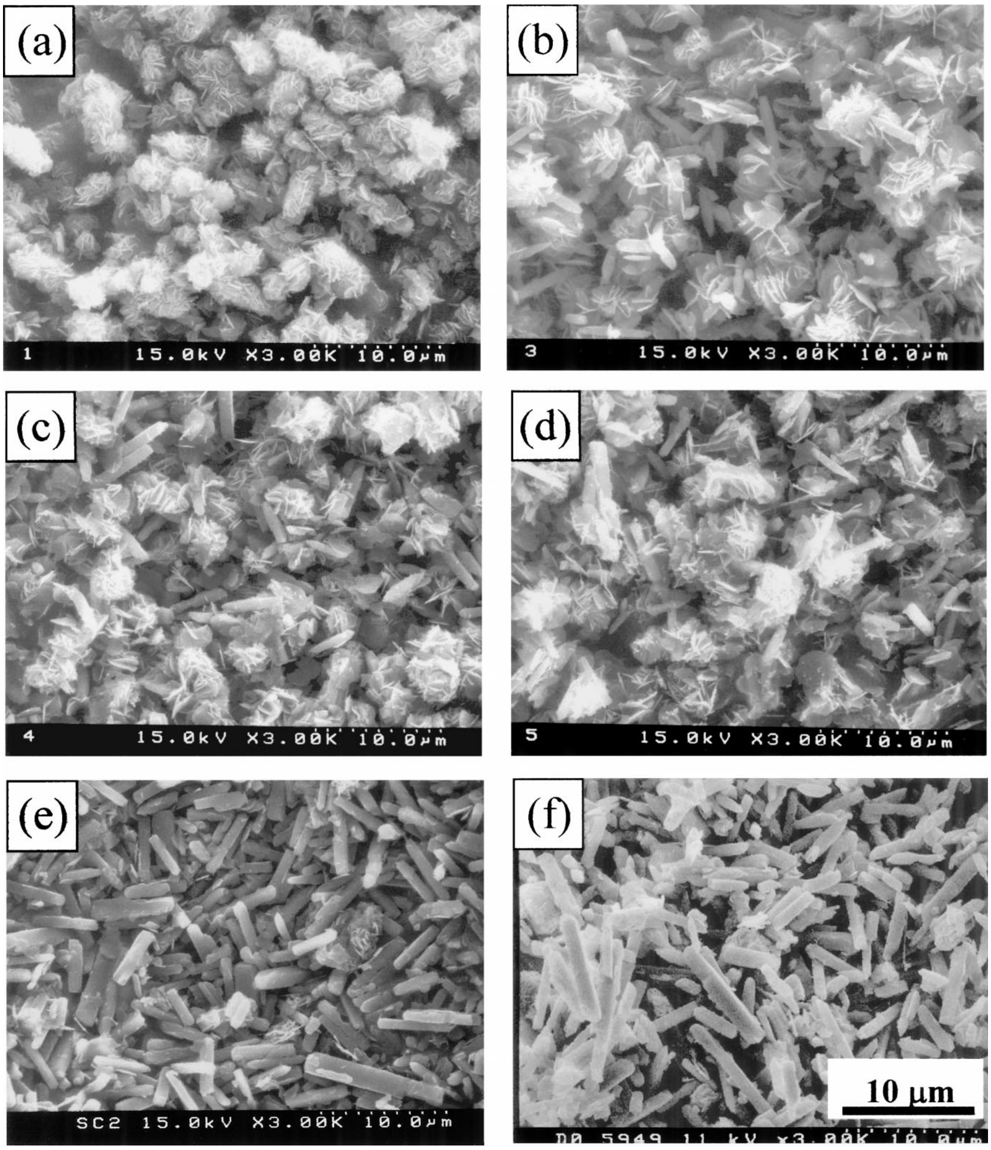

Figure 2 SEM micrographs of $LiAlO_2$ synthesized from reaction mixtures (50 mole % NaOH) with different mole ratios of $LiOH{\cdot}H_2O/\gamma$-Al_2O_3: (a) 2.0, (b) 4.0, (c) 5.0, (d) 6.0, (e) 7.0, and (f) 8.0.

rod-shapes as heat-treatment temperature increased. As seen in Fig. 4, the perfect rod-shaped β-$LiAlO_2$ with diameter of about 1 μm and length of about 10 μm could be obtained at 600 °C. However, it is very interesting that rod-shaped β-$LiAlO_2$ crystals transform totally into the γ-$LiAlO_2$ phase with a bipyramid crystal structure when being heat-treated at 700 °C, higher than the phase transition (β phase $\rightarrow \gamma$ phase) temperature of 650 °C. The optimum temperature for synthesizing rod-shaped β-$LiAlO_2$ crystals with a large aspect ratio was fixed as 600 °C from Figs 3 and 4.

3.1.2. Aspect ratio of β-$LiAlO_2$ crystals

The aspect ratio (lateral length/diameter) of fibrous type materials is one of the most important factors governing the strength of the fiber-reinforced matrixes. The control of the aspect ratio, however, is not easy, particularly for very short fibrous materials directly synthesized through crystallizing, like the rod-shaped β-$LiAlO_2$ particles in this work. The morphology changes of rod-shaped particles synthesized at 600 °C from the reaction mixture with the $LiOH{\cdot}H_2O/\gamma$-Al_2O_3 mole ratio of 7.0 and the NaOH content of 30–60 mole % were observed (see Fig. 5) and the aspect ratios determined from SEM pictures are given in Fig. 6. As can be seen in Figs 5 and 6, the aspect ratio increases with the content of NaOH in the range of 0–50 mole %: in the case of 50 mole % the high aspect ratio of 6.0–12.0 (diameter of about 1 μm), which is considered to be suitable for reinforcing the matrix made of 2 μm γ-$LiAlO_2$ particles, could be obtained. When the NaOH content becomes 60 mole%, however, the excess NaOH prohibits the reaction/direct contact between LiOH and γ-Al_2O_3, and consequently $Li_2Al_4(CO_3)(OH)_{12}{\cdot}3H_2O$ is the main product: this was also observed when the content of $LiOH{\cdot}H_2O$ in the reaction mixture was not sufficient as explained in Fig. 2a.

The effects of heating rate and dwelling time at 600 °C on the morphology/aspect ratio of rod-shaped β-$LiAlO_2$ particles synthesized from the reaction mixture with the same mole ratio above and 50 mole% NaOH were analyzed by SEM. It was found that the aspect ratio was independent of the heating rate in the range of

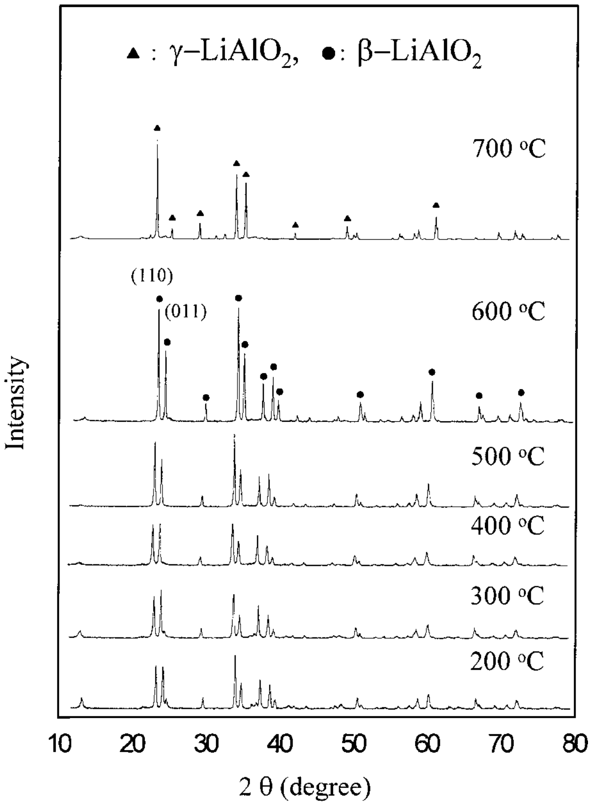

Figure 3 XRD patterns of $LiAlO_2$ synthesized at different temperatures.

1–5 °C/min. As a result, the faster heating rate, 5 °C/min was preferred in this work. Fig. 7 shows the linear increase of the aspect ratio with the dwelling time in the range of 2–10 h, while the aspect ratio has the almost constant value of 9–15 (average 12) after 10 h. It is concluded that the maximum aspect ratio being obtainable in this work was on average 12.

3.1.3. Synthesis of rod-shaped γ-$LiAlO_2$ particles

Since particles of γ-$LiAlO_2$ having the tetragonal structure are generally platelets or bipyramids in shape, it is well known that the γ-form can not easily be crystallized into rod-shapes unlike the β-form [1]. Therefore, the synthesis of rod-shaped γ-$LiAlO_2$ particles by the transformation of rod-shaped β-$LiAlO_2$ particles obtained in the preceding section to rod-shaped forms was tried, and the crystalline phase/shape of products was analyzed by XRD/SEM as given in Table III. The transformation of rod-shaped β-$LiAlO_2$ particles to the γ-phase was not observed around 700 °C but occurred completely or partly above 750 °C depending on the heat-treatment time and atmosphere (i.e., crucible closed with top-cover or open). The complete transformation of the β-phase to the γ-phase was observed even when the dwelling above 780 °C for a short

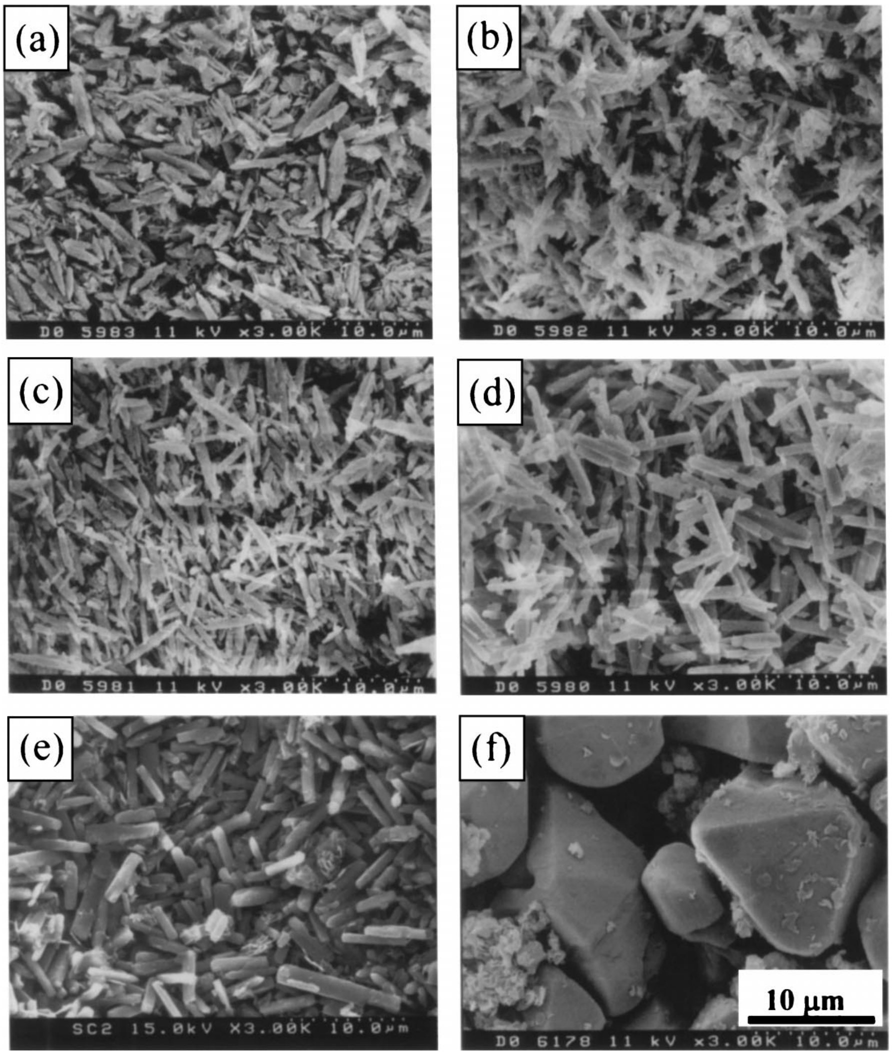

Figure 4 SEM micrographs of $LiAlO_2$ synthesized at different temperatures: (a) 200 °C, (b) 300 °C, (c) 400 °C, (d) 500 °C, (e) 600 °C, and (f) 700 °C.

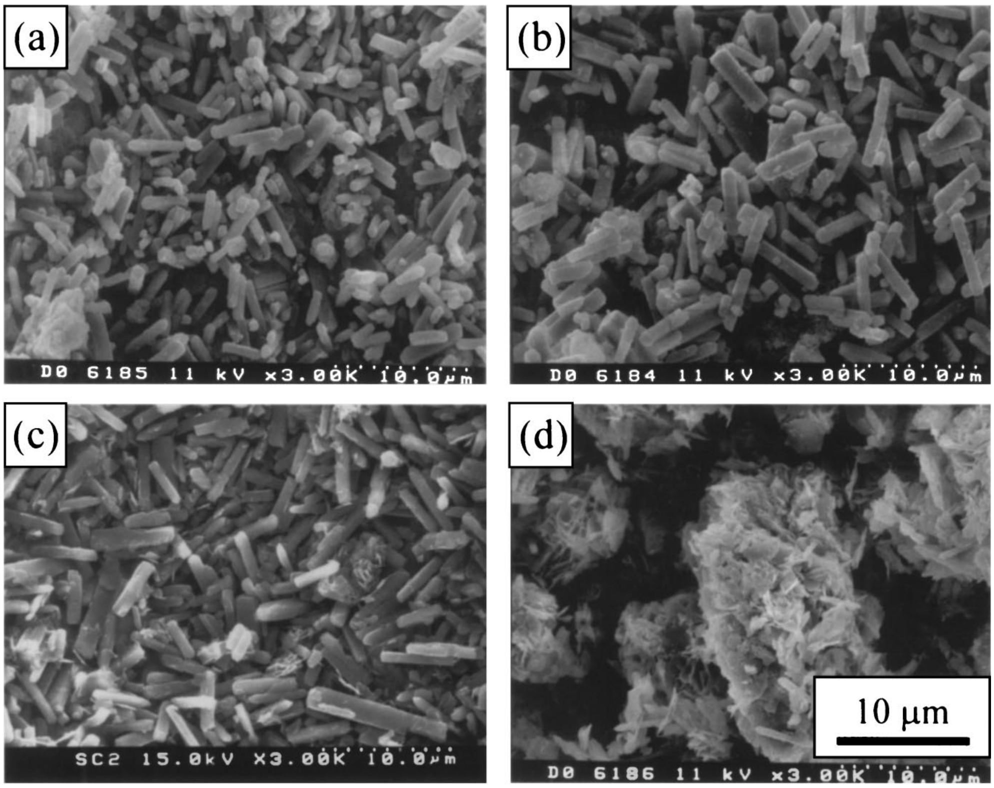

Figure 5 SEM micrographs of $LiAlO_2$ synthesized from reaction mixtures ($LiOH{\cdot}H_2O/\gamma$-Al_2O_3 mole ratio 7.0) with different mole % of NaOH: (a) 30, (b) 40, (c) 50, and (d) 60.

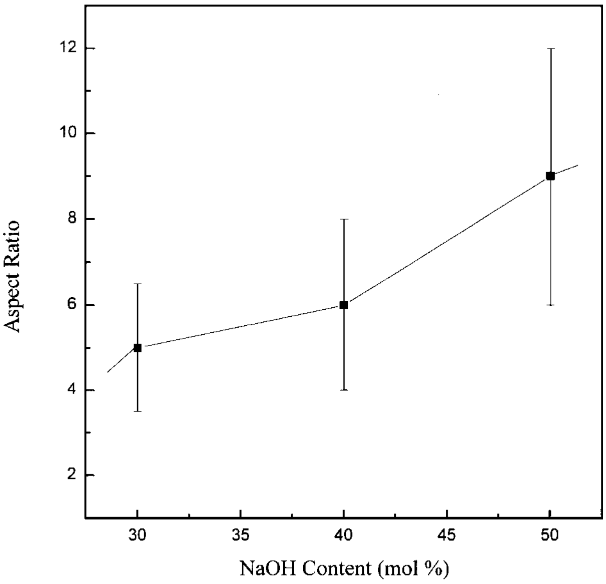

Figure 6 Variation of the aspect ratio of β-$LiAlO_2$ with the content of NaOH ($LiOH{\cdot}H_2O/\gamma$-Al_2O_3 mole ratio 7.0).

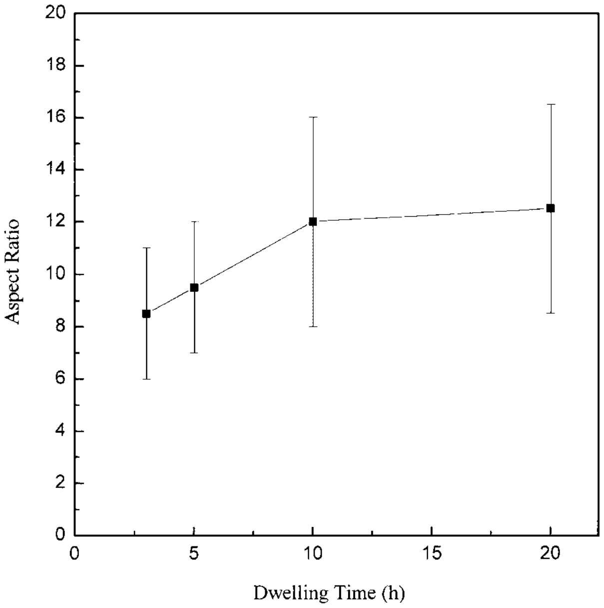

Figure 7 Variation of the aspect ratio of β-$LiAlO_2$ with the dwelling time at 600 °C.

period of 0.3–5 h in an open atmosphere, while the rod-shape morphology changed into the granular type unsuitable for the reinforcing process of the matrix. It was found that the crucible atmosphere was an important factor influencing the shape of particles as seen in Specimens No. 12 and 15 of Table III. Eventually, perfect rod-shaped γ-$LiAlO_2$ particles could be synthesized by heat-treating rod-shaped β-$LiAlO_2$ particles at 750 °C for more than 10 h in an open atmosphere (Specimen No. 7 in Table III) or by heat-treating at 800 °C for more than 3 h in a closed atmosphere (Specimens No. 15 and 16). The latter case, particularly the Specimen No. 15 case is the most desirable because of the short processing time.

3.2. Stability of rod-shaped $LiAlO_2$ in molten carbonates

The stability test was performed to verify whether the rod-shaped β- or γ-$LiAlO_2$ particles could be used as a reinforcing material in the MCFC atmosphere.

TABLE III Transformation of rod-shaped β-LiAlO$_2$ by heat-treatment

Specimen No.	Heat-treatment condition			Product	
	Temp. (°C)	Time (h)	Atmosphere*	Phase	shape**
1	700	3	Open	β	R
2	700	5	Open	β	R
3	700	10	Open	β	R
4	750	1	Open	$\gamma+\beta$	R
5	750	3	Open	$\gamma+\beta$	R
6	750	5	Open	$\gamma+\beta$	R
7	750	10	Open	γ	R
8	780	0.5	Open	γ	R + G
9	780	1	Open	γ	G
10	780	3	Open	γ	G
11	800	0.5	Open	γ	G
12	800	3	Open	γ	G
13	800	0.5	Closed	$\gamma+\beta$	R
14	800	1	Closed	$\gamma+\beta$	R
15	800	3	Closed	γ	R
16	800	10	Closed	γ	R

*Open: crucible cover open, Closed: Crucible cover closed.
**R: Rod type, G: Granule type.

Figs 8 and 9 show changes of the crystalline phase and morphology, respectively, with the corrosion testing time in molten carbonates at 650 °C for rod-shaped particles. A considerable portion of β-LiAlO$_2$ particles transformed into the γ-phase even when treated for 24 h, and it was found that only γ-LiAlO$_2$ particles existed after 240 h. At the same time, as seen in Fig. 9a, it should be noted that the rod-shape of the β-phase changed into the bipyramid shape of the typical γ-phase. This result indicates clearly that rod-shaped β-particles are not stable as a reinforcing material in the MCFC operation atmosphere. As seen from Figs 8b and 9b, however, the rod-shaped γ-LiAlO$_2$ particles did not show any phase and morphology changes although treated for 700 h. It is concluded that the rod-shaped γ-LiAlO$_2$ particle is very stable with alkali molten carbonates unlike the β-form.

3.3. Rod-shaped particle reinforced matrixes

3.3.1. Microstructures

The morphology change of the final matrix fabricated from the slurry containing 100% rod-shaped γ-LiAlO$_2$ particles with the slurry milling time was observed for optimizing the milling time. As seen in Fig. 10, milling for more than 3 d causes rod-shape particles to breakdown and their aspect ratio to decrease. This results in the reduction of the reinforcing efficiency: therefore, milling was conducted for 3 d in this work.

Fig. 11 shows the microstructures of the matrixes and the distribution of rod-shaped particles in the matrix depending on its content. It is observed that the matrix containing a small amount of the 10–30 wt % rod-shape particles has a non-oriented distribution like the 3-dimensional distribution. On the other hand, the 2-dimensional distribution in the x-y direction as seen in Fig. 11c–e occurs in matrixes containing more than 50% rod-shape particles. In general, in order to improve the flexural strength of tape-casted thin matrixes, the 2-d distribution of fibrous materials is much preferred, and consequently the suitable content of the rod-shaped particle was found to be more than 50 wt%.

In principle, the electrolyte content of molten carbonates in the MCFC matrix should be more than 50 vol%

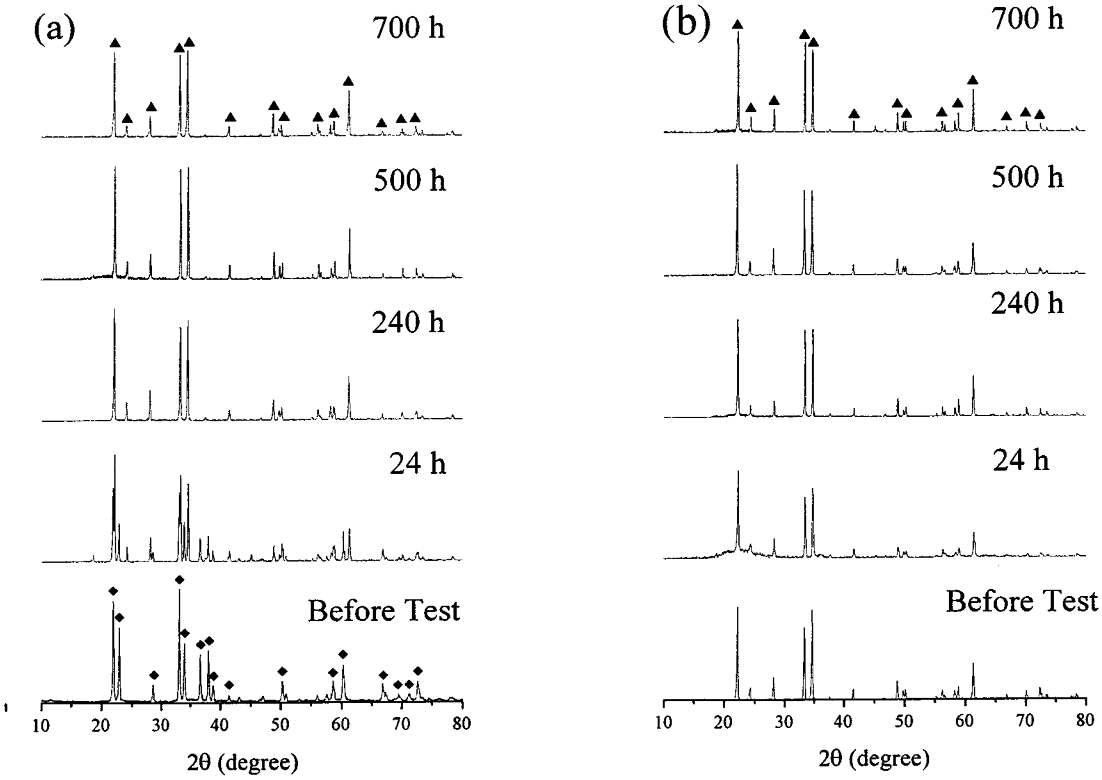

Figure 8 XRD patterns of LiAlO$_2$ particles treated with molten carbonates at 650 °C for 24–700 h: (a) β-LiAlO$_2$ particles and (b) γ-LiAlO$_2$ particles (◆: β-LiAlO$_2$, ▲: γ-LiAlO$_2$ phase).

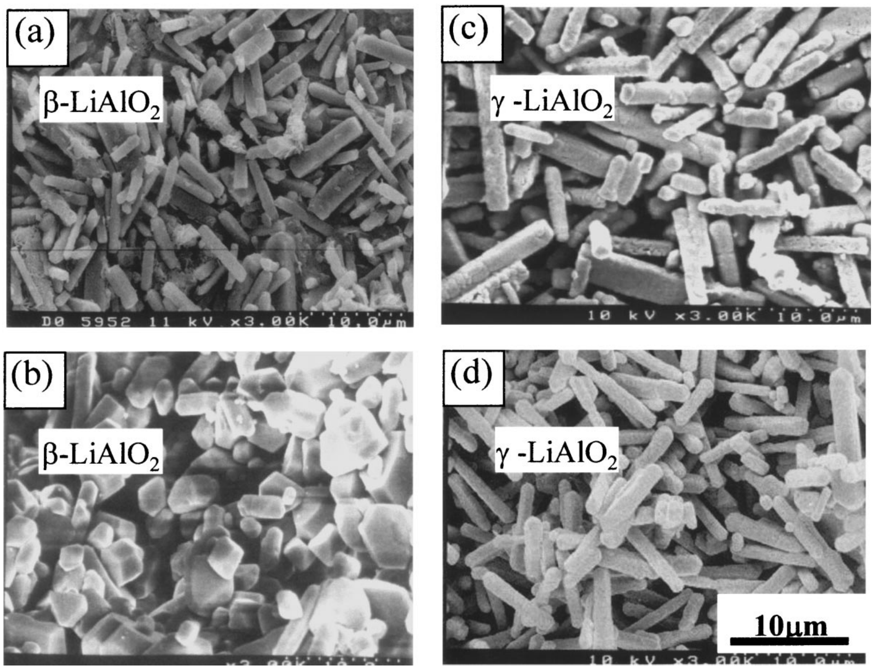

Figure 9 Morphology changes of LiAlO$_2$ particles treated with molten carbonates at 650 °C for 700 h: (a) untreated β-LiAlO$_2$, (b) treated β-LiAlO$_2$, (c) untreated γ-LiAlO$_2$, and (d) treated γ-LiAlO$_2$.

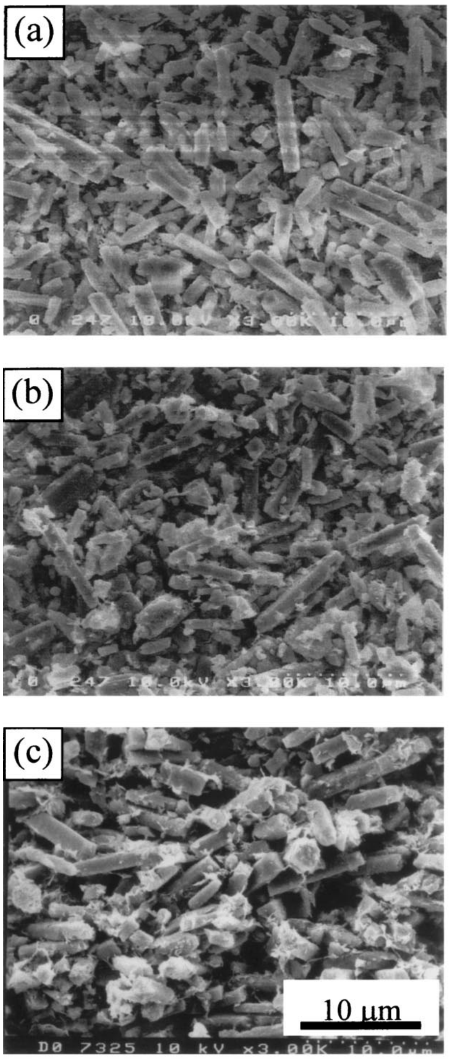

Figure 10 Morphology (fracture surface) changes of final γ-LiAlO$_2$ matrixes prepared from the slurry containing 100% rod-shaped γ-LiAlO$_2$ particles with ball milling time: (a) 3 d, (b) 4 d, and (c) 5 d.

and be very well retained in the matrix. The most important characteristics required in the matrix are therefore a porosity of 50–60% and a pore size of 0.1–0.3 μm [4, 13]. Fig. 12 shows that the pore volume does not much depend on the content of the rod-shaped particles and the approximate value is about 55%, slightly less than 60% of the matrix without the rod-shaped particles. It is also observed in Fig. 13 that the average pore size increased from 0.1 to 0.4 μm as the content of the rod-shaped particles increased from 10 to 100 wt%. The weighted pore size range in the matrix containing 50–70 wt% rod-shaped particles is 0.05–0.3 μm and is evaluated as a proper size range for the MCFC applications.

3.3.2. Mechanical strength of reinforced matrixes

For improving the mechanical strength of the matrix, the reinforcement by adding rod-shaped particles was carried out and the flexural strength of the reinforced matrixes were measured as given in Fig. 14. The maximum strength was obtained when adding 50 wt% rod-shaped particles, and its strength (197.6 g_f/mm^2) was increased more than twice as high as that of the non-reinforced matrix (91 g_f/mm^2). An increase in the matrix strength with the content of the rod-shaped particles was observed until 50 wt%, but over 50 wt% the strength was seen to decrease. This effect can be rationalized by the fact that the 2-d distribution due to the addition of a lot of rod-shaped particles as described in Fig. 11 might prevent cracks from propagating. In point of microstructures and the mechanical strength, the rod-shaped γ-LiAlO$_2$ particle is expected to be used as a useful reinforcing material in the MCFC matrix and its amount added for reinforcing was optimized to be 50 wt %.

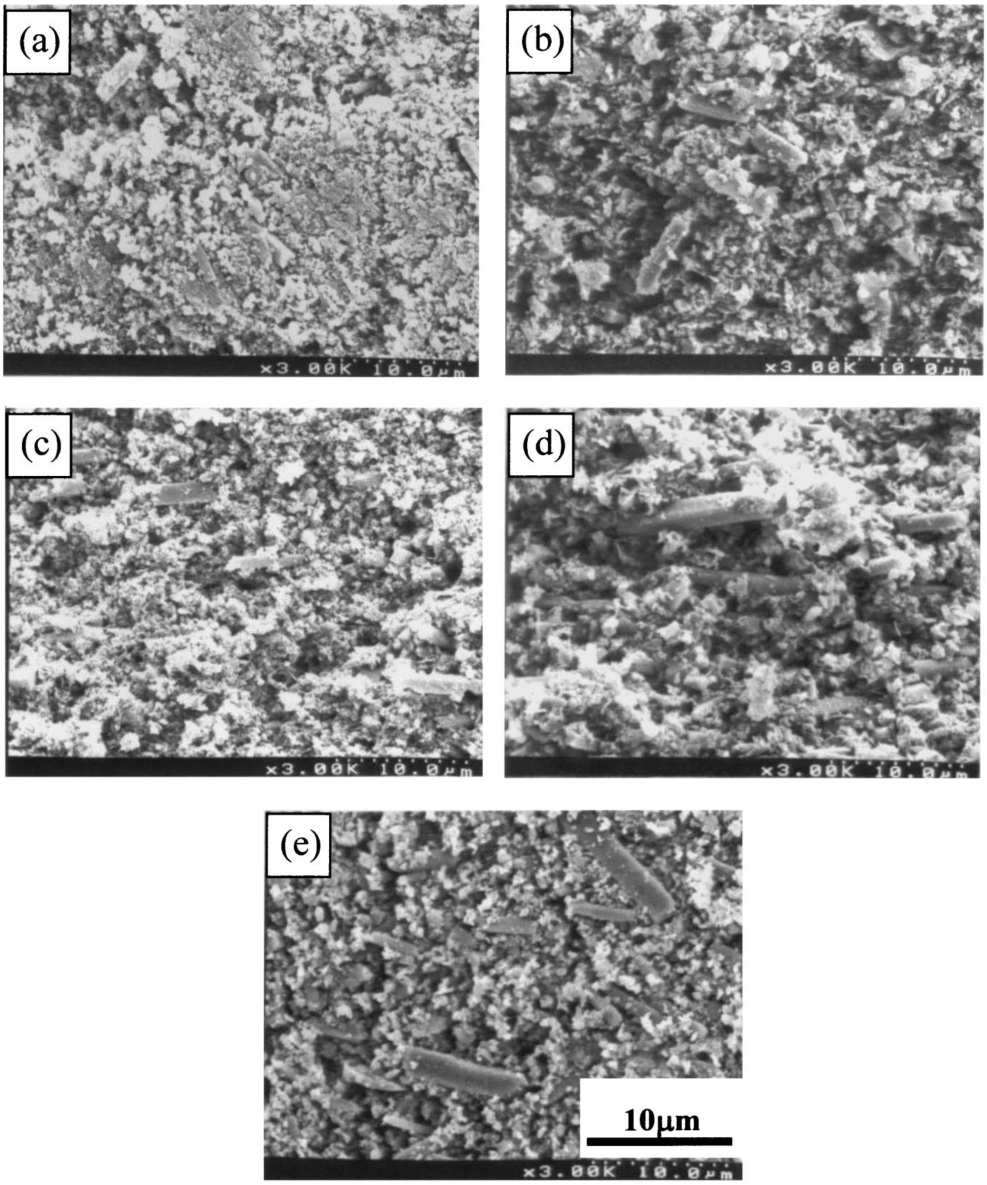

Figure 11 Morphology changes of (a)–(d) fracture surfaces and (e) top surface of reinforced matrixes with the content of rod-shaped particles: (a) 10 wt %, (b) 30 wt %, (c) 50 wt %, (d) 70 wt %, and (e) 50 wt %.

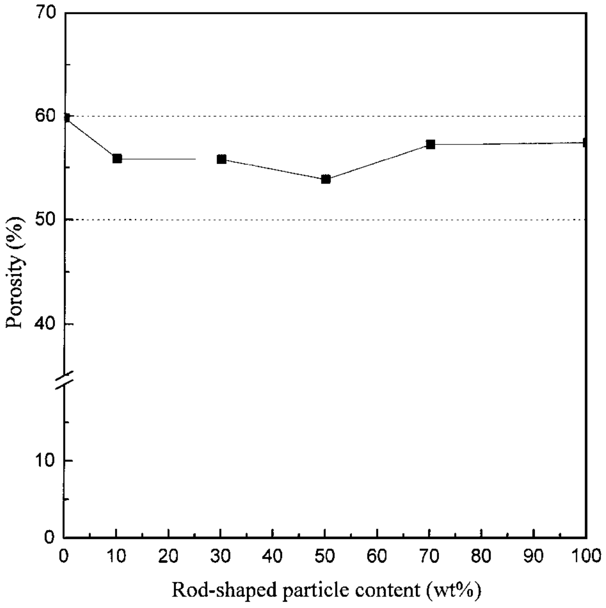

Figure 12 Porosity variation with the rod-shaped particle content.

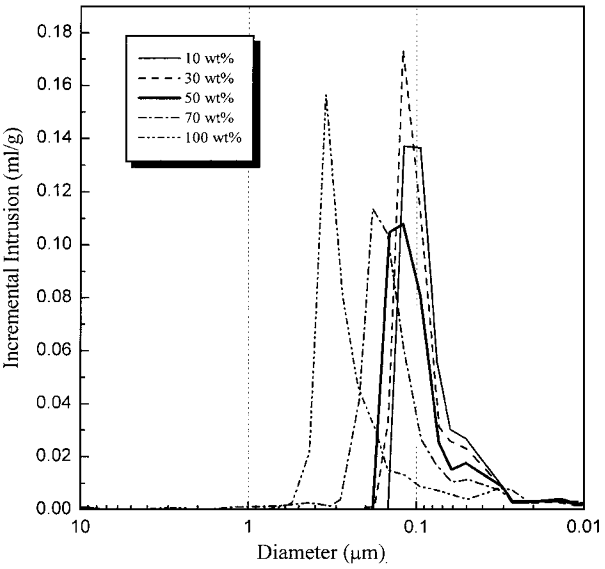

Figure 13 Pore size distribution vs rod-shaped particle content.

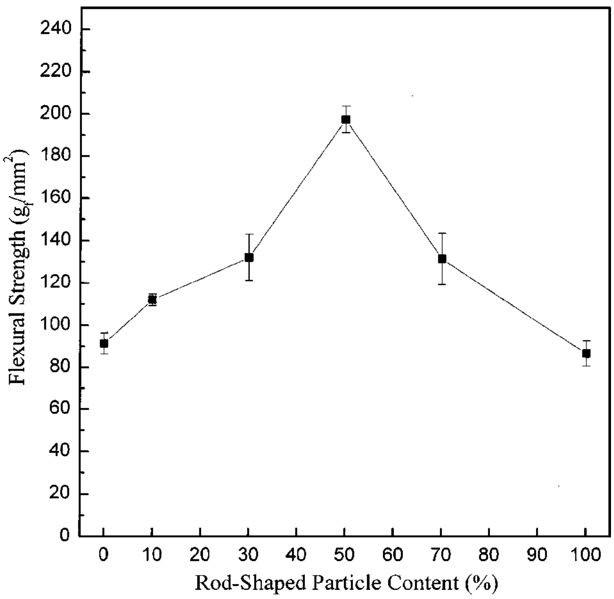

Figure 14 Flexural strength vs rod-shaped particle content.

4. Conclusions

The γ-$LiAlO_2$ matrix for MCFC could be greatly reinforced by adding rod-shaped γ-$LiAlO_2$ particles produced in this work. The main findings of this research are as follows:

1. Rod-shaped β-$LiAlO_2$ particles with the aspect ratio of 9–15 could be prepared by heat-treating the reaction mixture containing 50 mole % NaOH ($LiOH{\cdot}H_2O/\gamma$-Al_2O_3 mole ratio 7.0) at 600 °C for 10 h.

2. When rod-shaped β-$LiAlO_2$ particles were heat-treated at 750 °C for 10 h in open crucible or at 800 °C for 3 h in top-closed crucible, they completely transformed into γ-particles which maintained the same rod-shape morphology as the β-phase.

3. Rod-shaped γ-$LiAlO_2$ particles were found to be very stable in both the crystalline phase and the morphology with alkali molten carbonates at 650 °C for more than 700 h, while rod-shaped β-$LiAlO_2$ particles rapidly transformed into the bypiramid-shaped γ-particles.

4. The rod-shaped particle reinforced matrixes prepared by tape-casting of the slurry with the weight ratio 1.0 of rod-shaped γ-$LiAlO_2$ particles to commercial γ-$LiAlO_2$ particles (2.0 μm dia.) showed the average pore size of 0.12 μm and the porosity of 54% after being heat-treated at 650 °C for 2 h. It was found that the flexural strength (197 g_f/mm^2) of the reinforced matrix could be enhanced more than twice as much as that of the non-reinforced γ-$LiAlO_2$ matrix (91 g_f/mm^2).

Acknowledgements

This work was supported by Korea Electric Power Research Institute, 1997, Advanced Technology Project.

References

1. H. C. MARU, L. P. PAETSCH and A. PIGEAUD, in Proceedings of the Symposium on Molten Carbonate Fuel Cell Technology, edited by J. R. Selman and T. D. Claar (The Electrochemical Society Inc., Pennington, NJ, 1984) Vol. 84-13, p. 2.
2. H. C. MARU, M. FAROOQUE and A. PIGE, in Proceedings of the Second Symposium on Molten Carbonate Fuel Cell Technology, edited by J. R. Selman, D. A. Shores, H. C. Maru and I. Uchida (The Electrochemical Society Inc., Pennington, NJ, 1990) Vol. 90-16, p. 121.
3. P. A. LESSING, Z. Z. YANG, G. R. MILLER and H. YAMADA, *J. Electrochem. Soc.: Electrochemical Science and Technology* **135**(5) (1988) 1049.
4. C. ALVANI and E. RONCARI, High Temperature-High Pressure **20**(3) (1988) 247.
5. L. M. PAETSCH, J. D. DOYON and M. FAROOQUE, in Proceedings of the Symposium on Molten Carbonate Fuel Cell Technology, edited by D. Shores and H. Maru (The Electrochemical Society Inc., Pennington, NJ, 1993) Vol. 93-3, p. 88.
6. S. H. HYUN, S. A. HONG, W. S. KIM and H. C. SHIN, *J. Korean Ceram. Soc.* **31**(10) (1994) 1271.
7. S. H. HYUN, J. H. LEE and S. A. HONG, *ibid.* **33**(10) (1996) 1079.
8. H. OZU, Japanese Pat. 60,241,656 (1985).
9. K. SUZUKI, T. KAKIHARA, Y. YAMAMASU and T. SASA, in Mat. Res. Soc. Symp. Pro., 1995, Vol. 371, p. 297.
10. G. SAEKI, H. TAKAHASHI and A. WATANABE, *J. Cerm. Soc. Japan* **104**(3) (1996) 221.
11. K. KINOSHITA, J. W. SIM and J. P. ACKERMAN, *Mat. Res. Bull.* **13** (1978) 445.
12. G. SAEKI and A. WATANABE, *J. Ceram. Soc. Japan* **100**(12) (1992) 1421.
13. S. H. HYUN, K. H. BAEK and S. A. HONG, *J. Korean Ceram. Soc.* **34**(3) (1997) 303.
14. S. H. HYUN, S. C. CHO and S. A. HONG, *ibid.* **36**(2) (1999) 107.

Received 7 October 1999
and accepted 30 May 2000